Electronic Supplementary Material (ESI) for Dalton Transactions.


# Supporting Information

# $MnO_xH_y$-modified CoMoP/NF nanosheet arrays as hydrogen evolution reaction and oxygen evolution reaction bifunctional catalysts under alkaline condition

Xuemin Wang, Ke Zhang, Yuhan Xie, Dehua Yu, Haoze Tian and Yongbing Lou*

School of Chemistry and Chemical Engineering, Southeast University, Nanjing, 211189, P. R. China. E-mail: lou@seu.edu.cn.

# List of figures and tables

**Figure S13.** XPS of $MnO_xH_y$/CoMoP/NF as HER cathode and OER anode after 24 h stability treatment.

**Figure S14.** XRD of $MnO_xH_y$/CoMoP/NF as HER cathode and OER anode after 24 h stability treatment.

**Table S1.** The mass of of the as-synthesized catalysts.

**Table S2.** EIS equivalent circuit fitting results of catalysts under HER condition.

**Table S3.** EIS equivalent circuit fitting results of catalysts under OER condition.

**Table S4.** HER activity comparison of different catalysts in alkaline condition.

**Table S5.** OER activity comparison of different catalysts in alkaline condition.

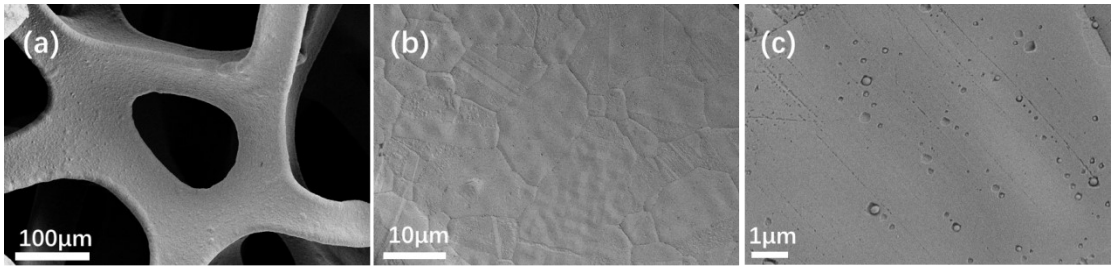


**Figure S1.** (a) SEM of bare NF at 100 μm size; (b) SEM of bare NF at 10 μm size; (c) SEM of bare NF at 1μm size.

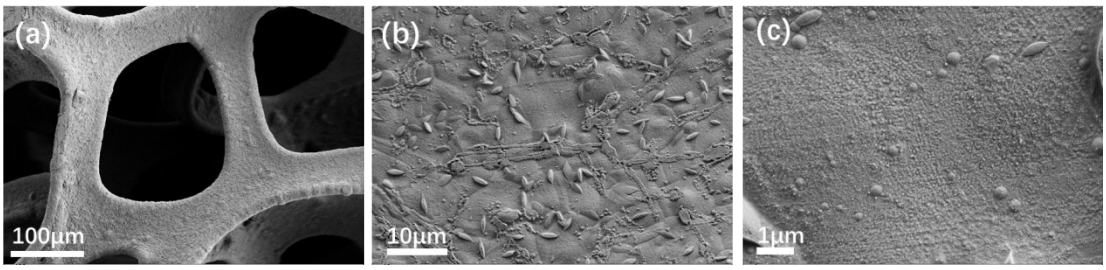


**Figure S2.** (a) SEM of $MnO_xH_y$/NF at 100 μm size; (b) SEM of $MnO_xH_y$/NF at 10 μm size; (c) SEM of $MnO_xH_y$/NF at 1 μm size.

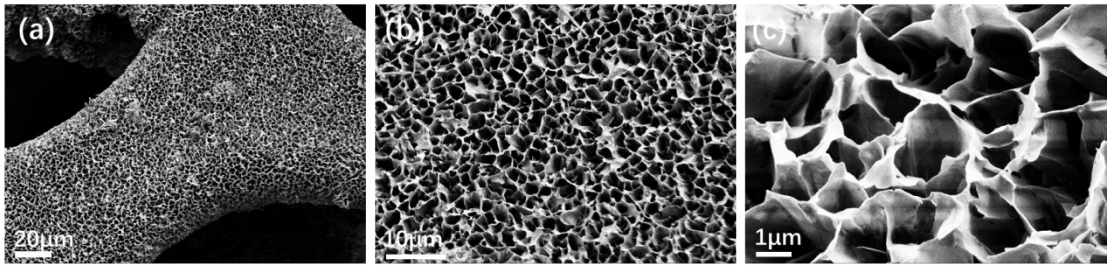


**Figure S3.** (a) SEM of CoMo precursors/NF at 20 μm size; (b) SEM of CoMo precursors/NF at 10 μm size; (c) SEM of CoMo precursors/NF at 1 μm size.

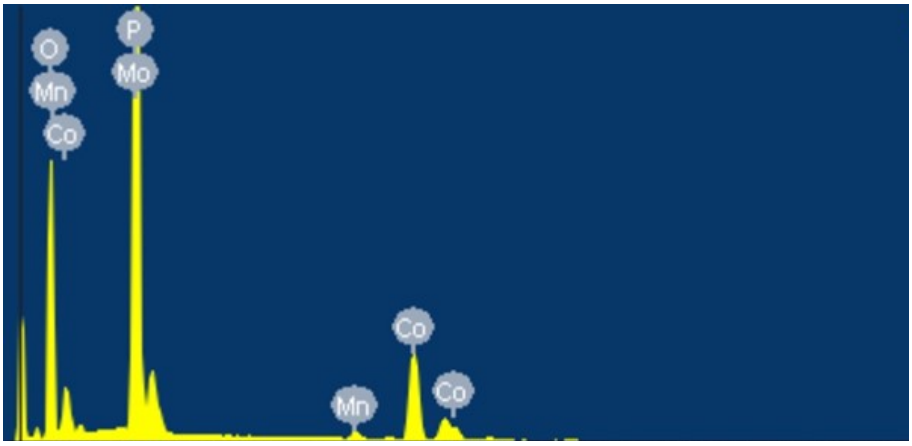


**Figure S4.** SEM-EDS spectra of $MnO_xH_y$/CoMoP/NF.

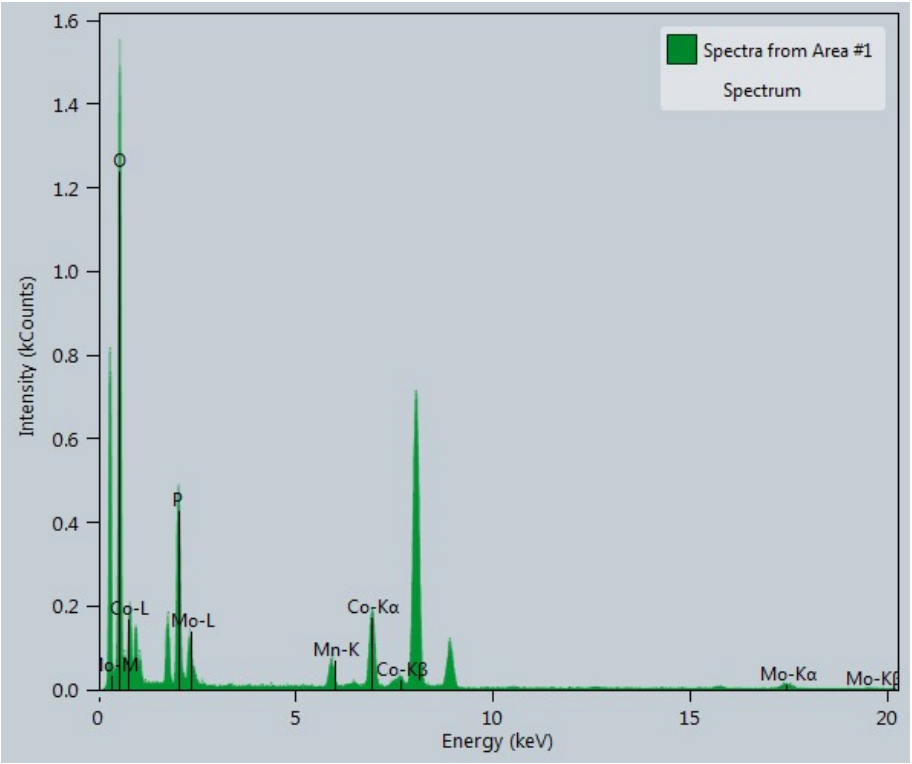


**Figure S5.** TEM-EDS spectra of $MnO_xH_y$/CoMoP/NF.

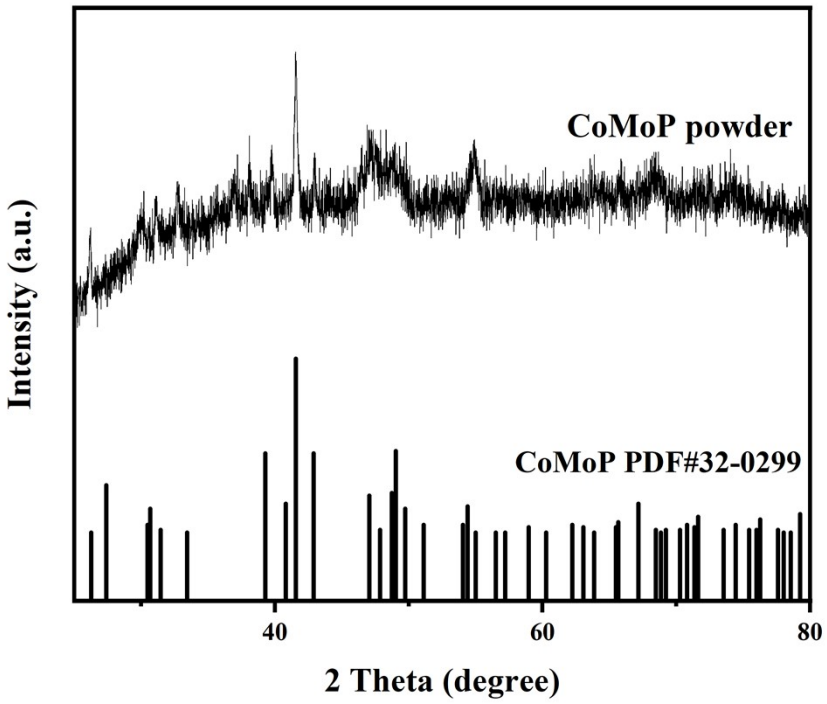


**Figure S6.** XRD of CoMoP powder.

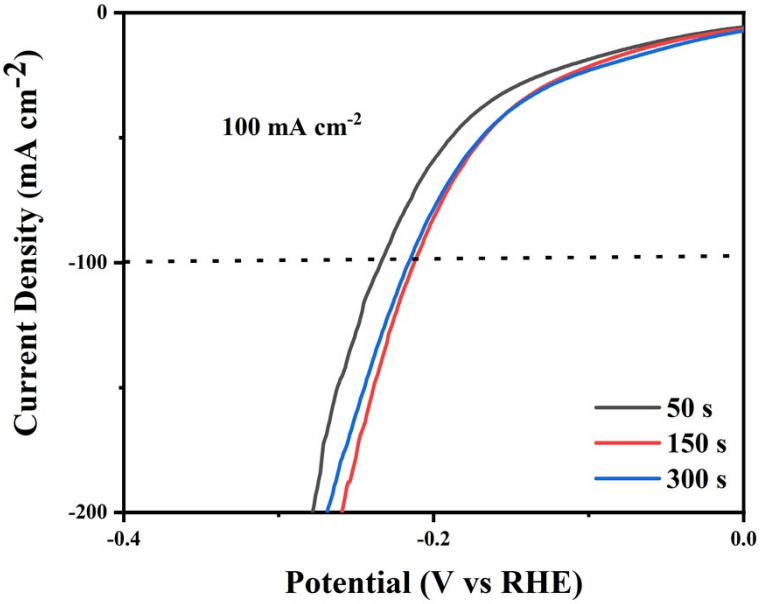


**Figure S7.** HER LSV curves of $MnO_xH_y$/CoMoP/NF with different electrodeposition times.

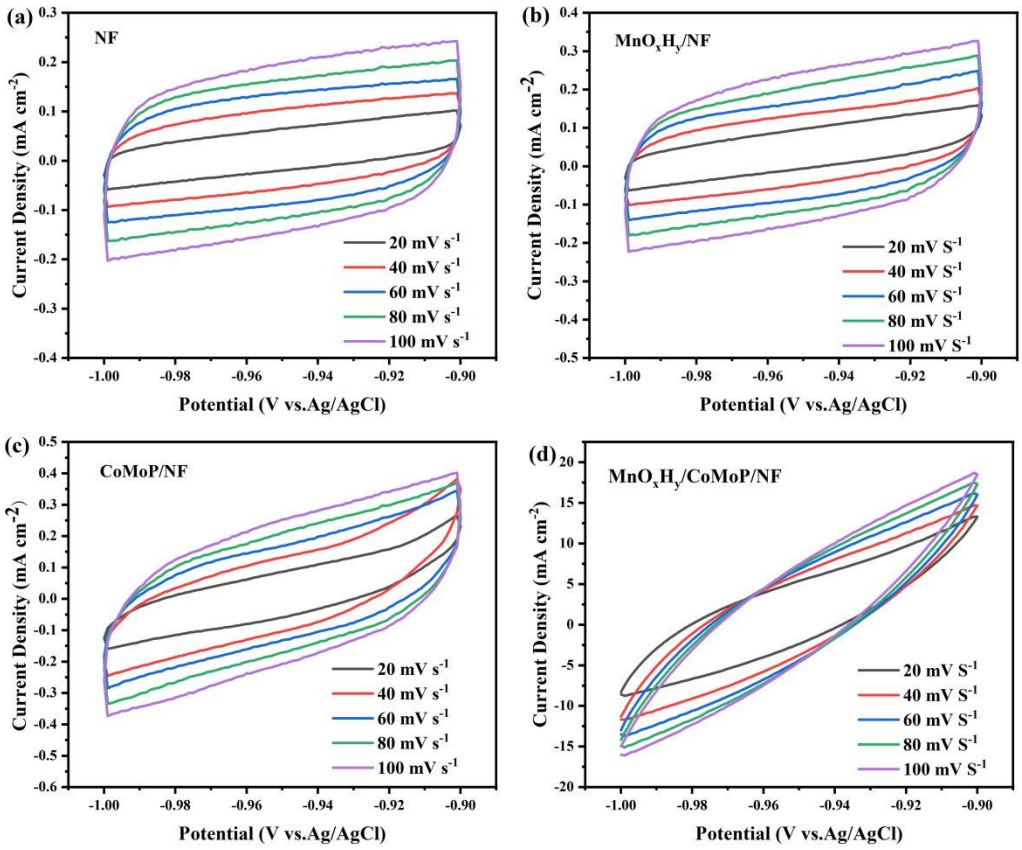


**Figure S8.** CV curves of NF, $MnO_xH_y$/NF, CoMoP/NF, and $MnO_xH_y$/CoMoP/NF in the voltage range of -1.0V to -0.9V (V vs Ag/AgCl).

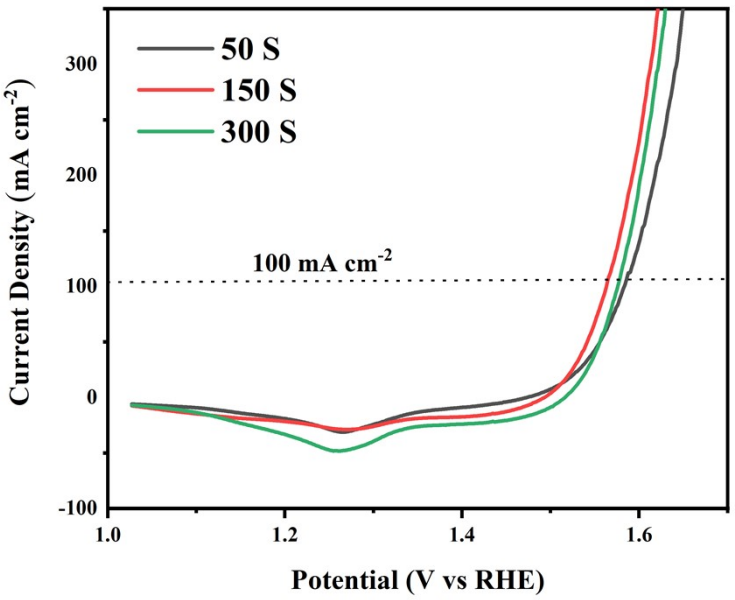


**Figure S9.** OER LSV curves of $MnO_xH_y$/CoMoP/NF with different electrodeposition times.

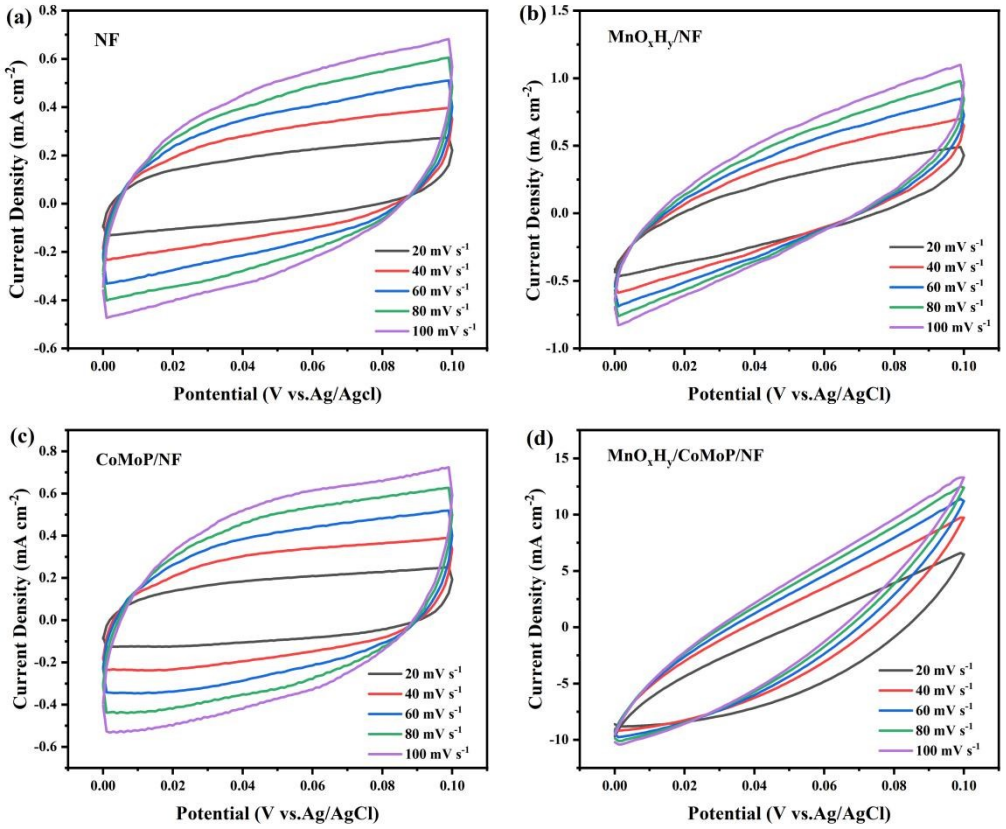


**Figure S10.** CV curves of NF, $MnO_xH_y$/NF, CoMoP/NF, and $MnO_xH_y$/CoMoP/NF in the voltage range of 0-0.1V (V vs Ag/AgCl).

## TOF calculation

The turnover frequency ($S^{-1}$) can be estimated according to this equation[2]:

TOF ($S^{-1}$) = $I/2n$F (HER); TOF ($S^{-1}$) = $I/4n$F (OER)

where $I$ represents the current density for different samples during the LSV measurement in 1 M KOH, F is the Faraday constant (C/mol), and $n$ is the number of the active sites (mol) for different samples. The number of active sites ($n$) was

measured from CV curves within the potential range of -0.2 to 0.6 V (vs. RHE) at a scan rate of 50 mV/s in 1.0 M PBS (pH=7).

n (mol) could be determined with the following equation:

$n$ (mol) = $Q$/2F (HER); $n$ (mol) = $Q$/4F (OER)

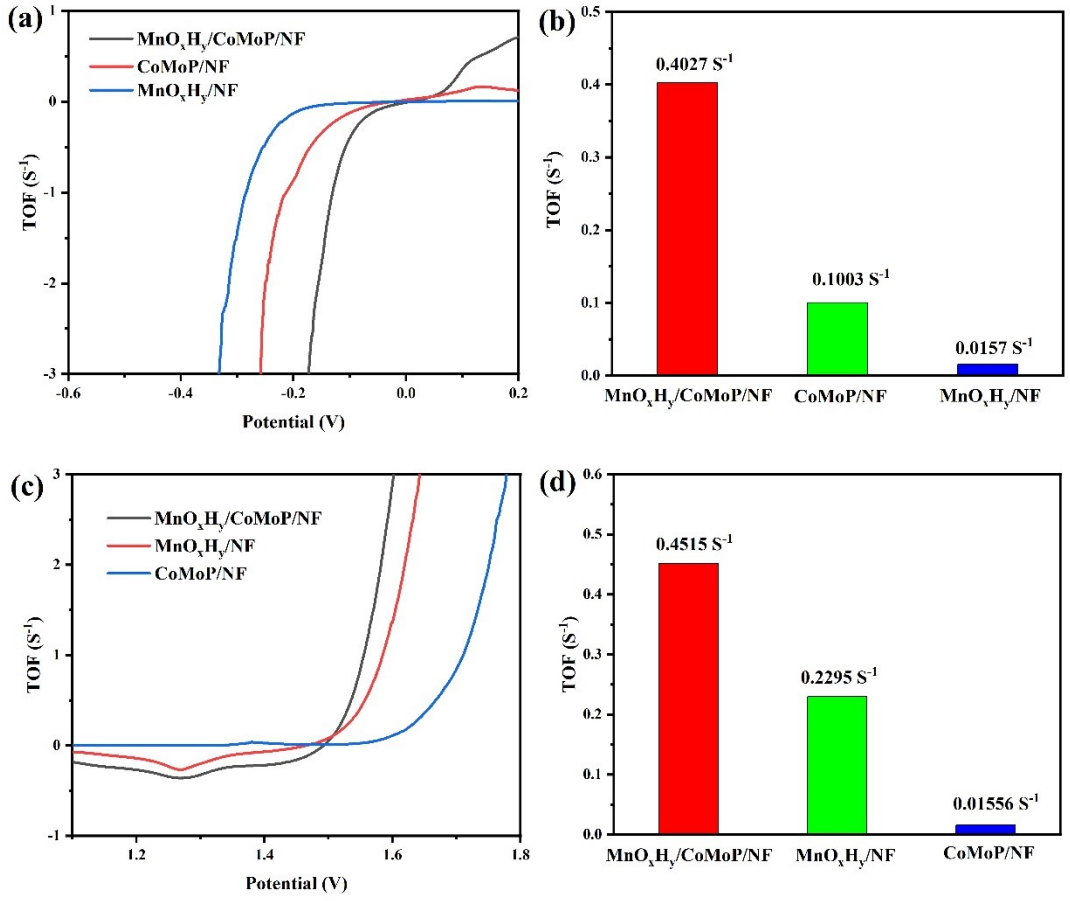


**Figure S11.** (a) Calculated TOFs for the as-synthesized catalysts in 1 M KOH (for HER); (b) TOF values of the as-synthesized catalysts at the overpotential of 100 mV (for HER); (c) Calculated TOFs for the as-synthesized catalysts in 1 M KOH (for OER); (d) TOF values of the as-synthesized catalysts at the overpotential of 300 mV (for OER).

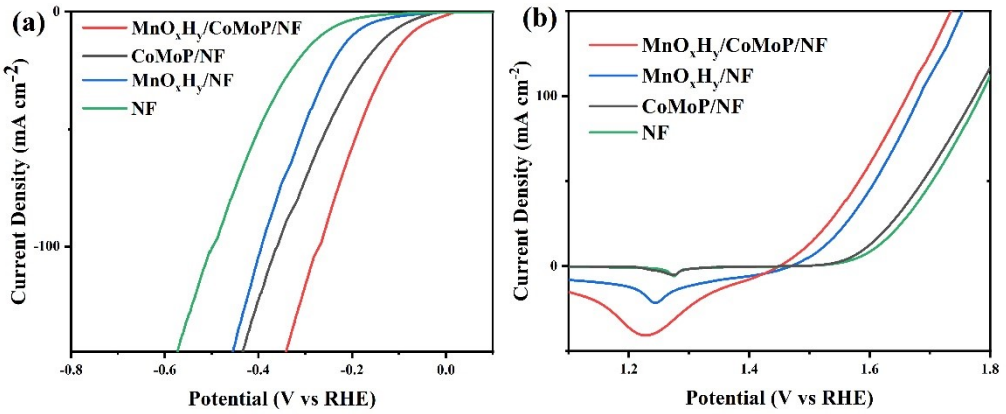


**Figure S12.** (a) Electrocatalytic HER LSV (without IR-correction, Speed of 5 mV $s^{-1}$) performance of $MnO_xH_y$/CoMoP/NF, CoMoP/NF, $MnO_xH_y$/NF and bare NF in 1 M KOH; (b) Electrocatalytic OER LSV (without IR-correction, Speed of 5 mV $s^{-1}$) performance of $MnO_xH_y$/CoMoP/NF, CoMoP/NF, $MnO_xH_y$/NF and bare NF in 1 M KOH.

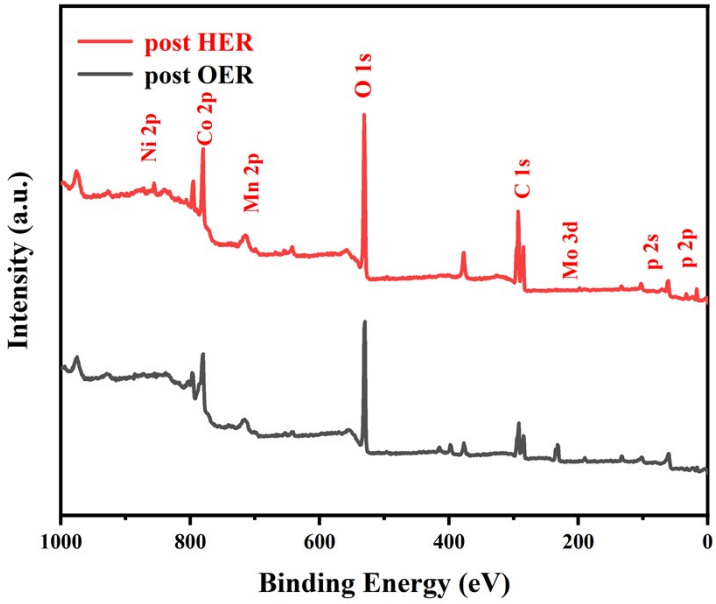


**Figure S13.** XPS of $MnO_xH_y$/CoMoP/NF as HER cathode and OER anode after 24 h stability treatment.

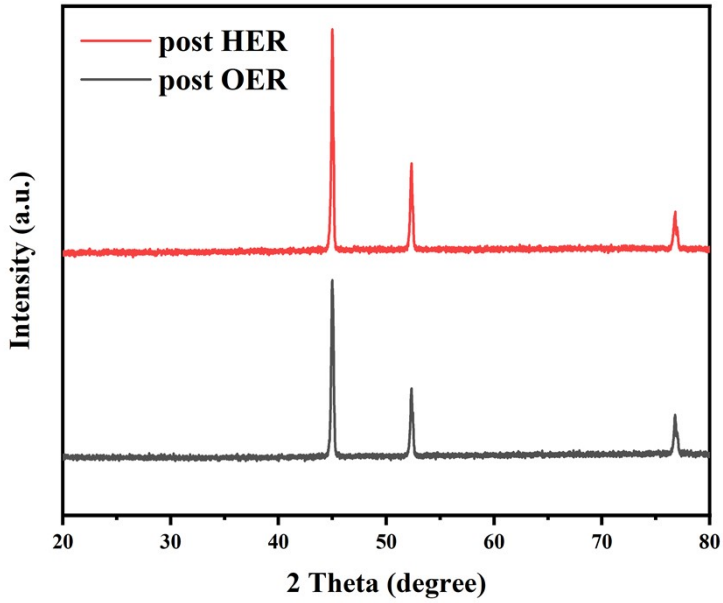


**Figure S14.** XRD of $MnO_xH_y$/CoMoP/NF as HER cathode and OER anode after 24 h stability treatment.

**Table S1.** The mass of of the as-synthesized catalysts.

| Samples | area | mass | Δm |
|---|---|---|---|
| NF | 1*1cm$^{-2}$ | 63.4 mg | — |
| CoMoP/NF | 1*1cm$^{-2}$ | 87.6 mg | 24.2 mg |
| $MnO_xH_y$/CoMoP/NF | 1*1cm$^{-2}$ | 94.5 mg | 6.9 mg |

**Table S2.** EIS equivalent circuit fitting results of catalysts under HER condition.

| Cathodes | $R_{ct}$ (Ω) |
|---|---|
| **$MnO_xH_y$/CoMoP/NF** | 3.56 |
| **CoMoP/NF** | 8.86 |
| **$MnO_xH_y$/NF** | 9.88 |

**Table S3.** EIS equivalent circuit fitting results of catalysts under OER condition.

| Cathodes | $R_{ct}$ (Ω) |
|---|---|
| **$MnO_xH_y$/CoMoP/NF** | 0.89 |
| **$MnO_xH_y$/NF** | 2.67 |
| **CoMoP/NF** | 3.68 |

**Table S4.** HER activity comparison of different catalysts in alkaline condition.

| Catalyst | Electrolyte | Current density | Overpotential | Reference |
|---|---|---|---|---|
| $MnO_xH_y$/CoMoP/NF | 1M KOH | 10 mA/cm$^2$ | 61 mV | This work |
| $MnO_xH_y$/CoMoP/NF | 1M KOH | 100 mA/cm$^2$ | 138 mV | This work |
| Ce-CoMoP/MoP/C | 1M KOH | 10 mA/cm$^2$ | 188 mV | 1 |
| One-Dimensional CoMoP Nanostructures | 1M KOH | 10 mA/cm$^2$ | 126 mV | 2 |
| Mn-CoP/$Co_2P$ | 1M KOH | 10 mA/cm$^2$ | 82 mV | 3 |
| Mn doped $Ni_2P$ | 1M KOH | 100 mA/cm$^2$ | 205 mV | 4 |
| $Mn_{0.52}Fe_{0.71}$Ni-MOF-74 | 1M KOH | 100 mA/cm$^2$ | 267 mV | 5 |
| $Ni_3S_2$/CoMoP/NF | 1M KOH | 10 mA/cm$^2$ | 96.8 mV | 6 |
| CoP/CoMoP/NF | 1M KOH | 100 mA/cm$^2$ | 250 mV | 7 |
| $Ni_2P$-MoP | 1M KOH | 100 mA/cm$^2$ | 161 mV | 8 |

**Table S5.** OER activity comparison of different catalysts in alkaline condition.

| Catalyst | Electrolyte | Current density | Overpotential | Reference |
|---|---|---|---|---|
| $MnO_xH_y$/CoMoP/NF | 1M KOH | 100 mA/cm$^2$ | 330 mV | This work |
| One-Dimensional CoMoP Nanostructures | 1M KOH | 10 mA/cm$^2$ | 391 mV | 2 |
| FeMnZn/Mn-FeS | 1M KOH | 100 mA/cm$^2$ | 390 mV | 9 |
| $Mn_{0.52}Fe_{0.71}$Ni-MOF-74 | 1M KOH | 100 mA/cm$^2$ | 462 mV | 5 |
| $Ni_3S_2$/CoMoP/NF | 1M KOH | 50mA/cm$^2$ | 270 mV | 6 |
| CoP/MoP@C,N | 1M KOH | 100mA/cm$^2$ | 390 mV | 10 |
| CoMoP@N-doped CQDs | 1M KOH | 100 mA/cm$^2$ | 370 mV | 11 |
| CoMoP@N,P,C | 1M KOH | 10 mA/cm$^2$ | 296 mV | 12 |
| $Ni_2P$-MoP | 1M KOH | 10 mA/cm$^2$ | 319 mV | 8 |

## Reference


1. T. Chen, Y. Fu, W. Liao, Y. Zhang, M. Qian, H. Dai, X. Tong and Q. Yang, *Energy Fuels*, 2021, **35**, 14169-14176.
2. X. Chang, J. Yan, X. Ding, Y. Jia, S. Li and M. Zhang, *Nanomaterials (Basel)*, 2022, **12**, 3886.
3. F. Tang, Y. W. Zhao, Y. Ge, Y. G. Sun, Y. Zhang, X. L. Yang, A. M. Cao, J. H. Qiu and X. J. Lin, *J Colloid Interface Sci*, 2022, **628**, 524-533.
4. P. Xu, L. Qiu, L. Wei, Y. Liu, D. Yuan, Y. Wang and P. Tsiakaras, *Catal. Today*, 2020, **355**, 815-821.
5. W. Zhou, Z. Xue, Q. Liu, Y. Li, J. Hu and G. Li, *ChemSusChem*, 2020, **13**, 5647-5653.
6. M. B. Poudel, N. Logeshwaran, A. R. Kim, K. S.C, S. Vijayapradeep and D. J. Yoo, *J Alloy Compd*, 2023, **960**, 170678-170689.
7. D. Ma, Z. He, T. Wei, L. Wang, Y. Li, K. V. Yurievich, R. Anton, T. Bian and S. Yan, *Int. J. Hydrogen Energy*, 2023.
8. W. Zhang, H. Yan, Y. Liu, D. Wang, Y. Jiao, A. Wu, X. Wang, R. Wang and C. Tian, *J. Mater. Chem. A*, 2023, **11**, 15033-15043.
9. L. Huang, R. Yao, Z. Li, J. He, Y. Li, H. Zong, S. Han, J. Lian, Y.-G. Li and X. Ding, *Green Chem*, 2023, **25**, 4326-4335.
10. D. Sun, S. Lin, Y. Yu, S. Liu, F. Meng, G. Du and B. Xu, *J Alloy Compd*, 2022, **895**, 162595-162604.
11. J. Han, J. Wu, S. Guan, R. Xu, J. Zhang, J. Wang, T. Guan, Z. Liu and K. Li, *Electrochim. Acta*, 2023, **438**, 141595-141604.
12. L. Yu, Y. Xiao, C. Luan, J. Yang, H. Qiao, Y. Wang, X. Zhang, X. Dai, Y. Yang and H. Zhao, *ACS Appl. Mater. Interfaces*, 2019, **11**, 6890-6899.